Phys Chem Minerals (2004) 31: 329–336
DOI 10.1007/s00269-004-0387-x

ORIGINAL PAPER

N. Hirao · E. Ohtani · T. Kondo · T. Kikegawa

Equation of state of iron–silicon alloys to megabar pressure

Received: 18 May 2003 / Accepted: 2 February 2004

Abstract The stability and pressure–volume equation of state of iron–silicon alloys, Fe-8.7 wt% Si and Fe-17.8 wt% Si, have been investigated using diamond-anvil cell techniques up to 196 and 124 GPa, respectively. Angular–dispersive X-ray diffractions of iron–silicon alloys were measured at room temperature using monochromatic synchrotron radiation and an imaging plate (IP). A bcc–Fe-8.7 wt% Si transformed to hcp structure at around 16∼36 GPa. The high-pressure phase of Fe-8.7 wt% Si with hexagonal close-packed (hcp) structure was found to be stable up to 196 GPa and no phase transition of bcc–Fe-17.8 wt% Si was observed up to 124 GPa. The pressure–volume data were fitted to a third-order Birch–Murnaghan equation of state (BM EOS) with zero–pressure parameters: $V_0 = 22.2(8)$ Å^3, $K_0 = 198(9)$ GPa, and $K'_0 = 4.7(3)$ for hcp–Fe-8.7 wt% Si and $V_0 = 179.41(45)$ Å^3, $K_0 = 207(15)$ GPa and $K'_0 = 5.1(6)$ for Fe-17.8 wt% Si. The density and bulk sound velocity of hcp–Fe-8.7 wt% Si indicate that the inner core could contain 3–5 wt% Si.

Keywords Iron–silicon alloys · High pressure · X-ray diffraction · Equation of state

Introduction

Seismic data indicate that both inner and outer cores are less dense than pure iron at core pressures and temperatures (e.g., Jephcoat and Olson 1987; Mao et al. 1990; Fiquet et al. 2001). This suggests that one or more light elements are contained as iron compounds in the inner and outer cores. The preferred candidates for the light elements are sulfur, oxygen, carbon, silicon, and hydrogen (Jeanloz 1990; Poirier 1994; Hillgren et al. 2000). However, the identity and abundance of the light elements are unknown. To constrain the composition of the Earth's core, it is essential to determine the stability, composition, and EOS of the iron compounds at core pressures and temperatures. Silicon has long been a favorite light element because it is one of the most abundant elements in the Earth (Birch 1952; Ringwood 1959). Recent works indicate that mantle silicates react with liquid iron at the core–mantle boundary and iron-silicon alloy is formed as a reaction product (Knittle and Jeanloz 1991; Goarant et al. 1992; Song and Ahrens 1994). However, Dubrovinsky et al. (2003) showed that iron and SiO_2 did not react at the pressures of 85–140 GPa. The mantle of the Earth is depleted in silicon relative to CI chondritic material, which suggests the dominant light element in the core might be silicon (MacDonald and Knopoff 1958; Ringwood 1959; Wänke 1981; Allègre et al. 1995). A number of both experimental and theoretical studies have been made in order to estimate silicon solubility in iron under the core conditions, but these results are not consistent with each other and give varying values of 0–20 wt% of the silicon content in the core (e.g., Balchan and Cowan 1966; Poirier 1994; Allègre et al. 1995; Sherman 1997; Hillgren et al. 2000; Gessmann et al. 2001; Lin et al. 2003). These conflicting results make it difficult to determine the effect of silicon on the compressibility of iron-rich alloys. Previous studies on Fe–Si system up to the pressure of the core, 270 GPa, have been conducted by the shock compression method (Balchan and Cowan 1966) and there are no compressibility measurements for the Fe–Si system by the static compression method under the core conditions. EOS measurements have been made for iron–silicon alloys

N. Hirao (✉) · E. Ohtani · T. Kondo
Institute of Mineralogy, Petrology and Economic Geology, Faculty of Science, Tohoku University, Sendai, 980-8578, Japan
e-mail:hirao@ganko.tohoku.ac.jp
Tel.: +81-22-217-6672
Fax: +81-22-217-6675

T. Kikegawa
Photon Factory, High Energy Accelerator Research Organization, Tsukuba, 305-0801, Japan

with various compositions and have been restricted up to 60 GPa (Drickamer et al. 1966; Knittle and Williams 1995; Wood et al. 1995; Guyot et al. 1997; Zhang and Guyot 1999; Dobson et al. 2003; Lin et al. 2003). Therefore, it is difficult to extrapolate density to the core pressure. In this paper, we report the results of a room temperature compression study of iron–silicon alloys at pressures up to 196 GPa.

Experimental

Two powdered iron–silicon alloys, Fe-9 wt% Si and Fe-17 wt% Si (Goodfellow Co. Ltd.) were used for the starting materials. The electron microprobe analysis of these alloys showed that the samples contain 8.7 ± 0.3 wt% Si, and 17.8 ± 0.3 wt% Si, respectively. The powdered sample of Fe-8.7 wt% Si ($Fe_{84}Si_{16}$) has a body-centered cubic (bcc) structure similar to α-iron under ambient conditions. The lattice parameter and unit-cell volume of Fe-8.7 wt% Si measured with the X-ray diffractometer (RINT; Rigaku Co., Ltd.) are $a_0 = 2.8437(3)$ and $V_0 = 22.995(6)$ Å^3, which are in agreement with values obtained by Zhang and Guyot (1999); i.e., 2.8429(8) Å and 22.976(20) Å^3, respectively. Fe-17.8 wt% Si ($Fe_{70}Si_{30}$) has a cubic DO_3 structure like Fe_3Al, Fe_3Si, or Ni_3Sb, which is related to the $L2_1$ structure typical of Heusler alloys. The unit cell contains eight bcc cells. This structure is similar to B2 structure because atoms are ordering in both structures (Lin et al. 2003). The lattice parameter and unit-cell volume of Fe-17.8 wt% Si measured by a conventional powder X-ray diffraction method (M18XCE, Macscience) at the ambient condition are $a_0 = 5.6401(47)$ Å and $V_0 = 179.41(45)$ Å^3, respectively.

High pressure was generated by a Mao–Bell-type diamond-anvil cell (DAC) with beveled type-I diamond anvils. Four experimental runs were made for two iron–silicon alloys. For two runs of Fe-8.7 wt% Si, the sample was compressed using the beveled anvils with 0.15/0.45-mm and 0.10/0.30-mm culets. For two runs of Fe-17.8 wt% Si, beveled diamond anvils with 0.25/0.60-mm and 0.15/0.45-mm culets were used. The rhenium gaskets with an initial thickness of 250 μm were preindented to about 15–40 GPa. The sample was loaded directly into the hole of the rhenium gasket. No pressure-transmitting medium was used to obtain the maximum sample volume. Pressures were measured before and after each exposure by the ruby fluorescence method (Mao et al. 1978) and the averages of these values were used as pressure values. For one experimental run on Fe-8.7 wt% Si up to 196 GPa, powdered platinum black (99.9% purity) as an internal pressure standard was added to the sample. The (111), (200), and (220) diffraction lines of Pt were used to calculate the unit-cell volume, which was converted directly to pressures based on the equation of state by Holmes et al. (1989). The accuracy of the present platinum scale will be within a few percent (Mao et al. 1990; Dubrovinsky et al. 2000). All the experiments were carried out at room temperature.

In situ high-pressure X-ray powder diffraction experiments were performed at the BL13A and BL18C beamlines in the Photon Factory, High Energy Accelerator Research Organisation (KEK). The incident X-ray beams were monochromatized to wavelengths of 0.4256 and 0.4264 Å at the BL13A and 0.6196 Å at the BL18C, respectively. The angle-dispersive technique was employed in order to get high resolution of the diffraction data. The beam was collimated to a 30-μm square at BL13A and a diameter of 25 μm at BL18C, respectively. The exposure time was varied from 5 to 90 min, depending on the experimental pressure. The two-dimensional image data were collected by IP. The recorded images were integrated in order to obtain a conventional one-dimension diffraction spectrum as a function of 2θ. A diffraction of the silver standard was used to determine the wavelength and the distance between the sample and IP.

Results

Typical spectra for Fe-8.7 wt% Si under high pressures are shown in Fig. 1 and the unit-cell parameters are listed in Tables 1 and 2. The diffraction patterns of Fe-8.7 wt% Si indicate that it transforms from bcc phase into the bcc and hcp phases at 16 GPa and room temperature, and the phase transformation to the hcp phase was completed at 36 GPa, which is in good agreement with Lin et al. (2002). The (100), (101), (102), and (110)

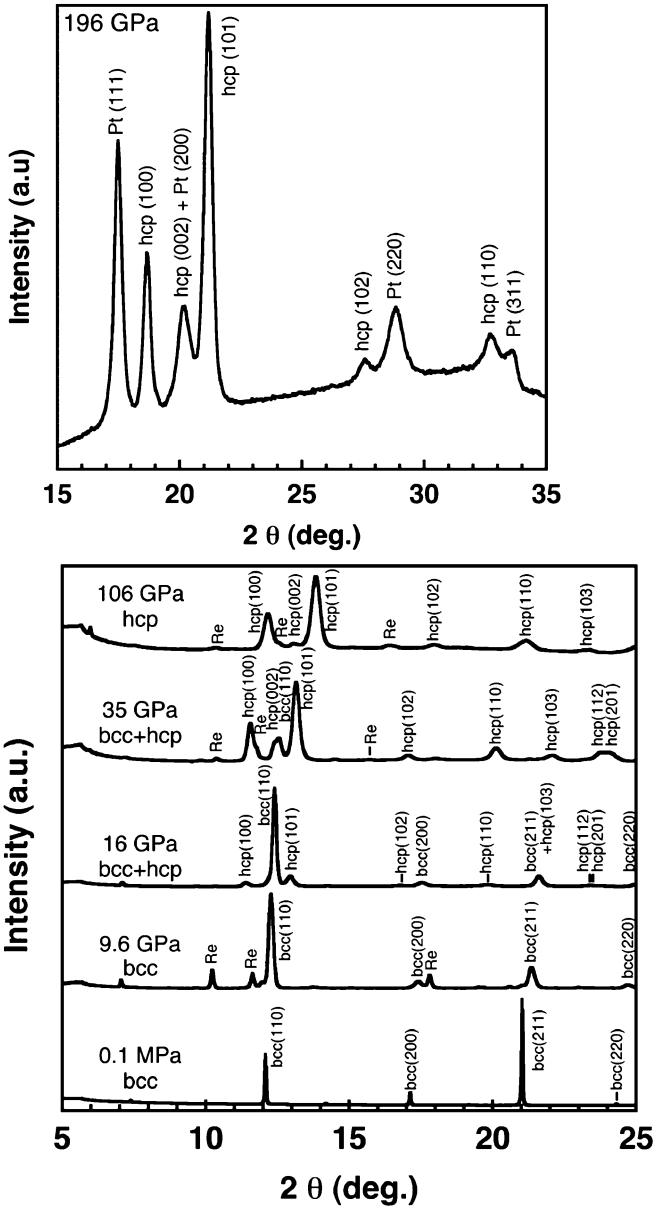

Fig. 1 Representative angle-dispersive X-ray diffraction spectra of Fe-8.7 wt% Si at different pressures and room temperature. A monochromatic beam (wavelength = 0.4264 Å) was used as X-ray source. *Re* indicates a diffraction line of the rhenium gasket (*lower*). The diffraction pattern recorded at 196 GPa using a monochromatic beam with a wavelength of 0.6196 Å (*upper*). *Pt* represents platinum for pressure standard

Table 1 Lattice parameters and volumes of bcc–Fe-8.7 wt% Si

P (GPa)	*a* (Å)	*V* (Å^3)
0.0	2.8437(3)	22.995(6)
1.4(1)[a]	2.838(1)	22.85(4)
2.1(2)[b]	2.841(1)	22.92(2)
3.7(2)[a]	2.838(2)	22.87(4)
5.4(1)[a]	2.826(1)	22.56(2)
7.3(3)[a]	2.8233(4)	22.506(10)
9.6(2)[a]	2.8135(2)	22.271(4)
11.1(2)[a]	2.8076(3)	22.13(1)
13.8(2)[a]	2.802(1)	22.00(2)
16.4(4)[a]	2.795(2)	21.83(5)
20.3(5)[a]	2.785(2)	21.59(4)
22.9(0)[b]	2.786(0)[c]	21.62(0)[c]
25.1(5)[a]	2.772(1)	21.29(2)
29.5(3)[a]	2.761(1)	21.04(1)
34.9(3)[c]	2.747(0)[c]	20.73(0)[c]

[a]First experiment
[b]Second experiment
[c]Error is zero because only one diffraction line could be observed

peaks from the hcp phase were observed and could be fitted to the highest pressure, indicating that the hcp phase is stable to at least 196 GPa. The (002) reflection was absent due to preferred orientation (Mao et al. 1990; Dubrovinsky et al. 1998). For Fe-17.8 wt% Si, no phase transition from the bcc structure was observed at pressures up to 124 GPa, the maximum pressure studied.

Table 2 Lattice parameters and volumes of hcp-Fe-8.7 wt% Si

P (GPa)	*a* (Å)	*c* (Å)	*V* (Å^3)	*c*/*a*
16.4(4)[a]	2.489(2)	4.083(1)	21.91(9)	1.640(1)
20.3(5)[a]	2.470(2)	3.998(5)	21.13(4)	1.618(1)
22.9(0)[b]	2.440(3)	3.901(11)	20.11(8)	1.599(3)
25.1(5)[a]	2.459(1)	3.969(4)	20.78(3)	1.614(1)
29.5(3)[a]	2.451(1)	3.947(3)	20.53(2)	1.610(1)
34.9(3)[a]	2.437(1)	3.928(3)	20.20(3)	1.612(1)
36.5(5)[b]	2.413(1)	3.852(4)	19.43(3)	1.596(1)
44.1(4)[a]	2.413(1)	3.874(3)	19.54(2)	1.605(1)
44.6(4.7)[b]	2.384(2)	3.798(7)	18.70(5)	1.593(2)
49.5(4)[a]	2.411(1)	3.857(4)	19.42(3)	1.600(1)
54.1(4)[a]	2.384(1)	3.831(3)	18.86(3)	1.607(1)
59.8(7)[a]	2.375(1)	3.810(3)	18.63(2)	1.604(1)
65.4(1)[a]	2.374(1)	3.810(3)	18.60(2)	1.605(1)
68.7(5)[a]	2.359(1)	3.783(2)	18.23(2)	1.603(1)
76.1(4)[a]	2.350(1)	3.771(3)	18.03(2)	1.605(1)
79.4(1.4)[b]	2.338(1)	3.727(5)	17.65(3)	1.594(1)
81.0(1)[a]	2.350(1)	3.769(3)	18.03(2)	1.603(1)
88.2(1)[a]	2.347(1)	3.754(3)	17.91(2)	1.599(1)
92.5(3)[a]	2.327(1)	3.733(3)	17.51(2)	1.604(1)
98.0(1.1)[a]	2.328(1)	3.727(3)	17.49(2)	1.601(1)
104.6(9)[b]	2.306(3)	3.686(11)	16.98(7)	1.598(3)
105.6(6)[a]	2.318(1)	3.725(4)	17.33(3)	1.607(1)
117.9(6)[b]	2.290(2)	3.661(7)	16.63(4)	1.599(2)
129.9(4.2)[b]	2.278(2)	3.647(6)	16.39(4)	1.601(2)
140.6(3.9)[b]	2.262(1)	3.635(2)	16.11(1)	1.607(1)
151.9(4.4)[b]	2.250(1)	3.616(2)	15.85(1)	1.607(1)
163.1(3.5)[b]	2.240(1)	3.603(4)	15.66(2)	1.608(1)
170.8(1.4)[b]	2.232(1)	3.592(3)	15.49(2)	1.609(1)
184.8(3.1)[b]	2.220(2)	3.575(5)	15.25(3)	1.610(2)
196.0(1.6)[b]	2.211(1)	3.564(4)	15.09(3)	1.612(1)
190.5(11.0)[b]	2.2120(2)	3.560(1)	15.086(4)	1.6095(2)

[a]First experiment
[b]Second experiment

The wide stability field of the bcc phase is in accord with the previous shock experiment (Balchan and Cowan 1966), indicating that Fe-19.8 wt% Si which has the same structure as Fe-17.8 wt% Si remained in the bcc structure up to 250 GPa. In Fe-17.8 wt% Si we could clearly observe the characteristic reflections for the DO_3 structure, (111), (311), and (511) up to 2 GPa, whereas (511) was observed at least up to 63 GPa. Therefore Fe-17.8 wt% Si possesses the DO_3 structure at least up to 63 GPa. Above this pressure, we could not detect the peak due to the limitation of the opening angle of the diamond-anvil cell ($2\theta > 26°$). Only the reflections of the B2 phase were detected from 63 to 124 GPa, the maximum pressure studied. Therefore it is difficult to conclude whether the alloy has DO_3 or B2 structure at pressures above 63 GPa.

The compression data for iron–silicon alloys, bcc Fe-8.7 wt% Si, hcp Fe-8.7 wt% Si, and Fe-17.8 wt% Si, are presented in Tables 1, 2, and 3, respectively. Compression curves derived from these experiments are plotted in Fig. 3 together with the data reported by Lin et al. (2003). Two iron–silicon alloys appear to be less compressible in these experiments, compared with Lin et al. (2003). To determine the elastic parameters, the pressure–volume data were fitted to the third-order BM EOS (Birch 1952). The EOS parameters obtained by the least-squares calculation are shown in Table 4. For the hcp phase of Fe-8.7 wt% Si, we made two runs. There are differences between the *P*–*V* data of our first and second runs. The results of the first run are not consistent with

Table 3 Lattice parameters and volumes of Fe-17.8 wt% Si

P (GPa)	*a* (Å)	*V* (Å^3)
0.0	5.640(5)	179.4(5)
0.4(0)[a]	5.607(2)	176.3(2)
0.5(4)[bc]	5.621(3)	177.6(3)
1.4(3)[a]	5.603(1)	175.9(1)
9.2(1)[a]	5.562(3)	172.0(2)
10.9(3)[bc]	5.557(2)	171.6(2)
13.0(3)[b]	5.553(2)	171.3(2)
13.7(3)[b]	5.551(3)	171.0(3)
14.7(4)[a]	5.544(3)	170.4(3)
15.7(3)[bc]	5.535(3)	169.6(3)
16.2(3)[bc]	5.530(2)	169.1(2)
20.3(3)[bc]	5.504(2)	166.8(2)
21.1(4)[a]	5.496(6)	166.0(6)
28.1(3)[bc]	5.455(2)	162.3(2)
30.6(3)[a]	5.432(3)	160.3(3)
40.0(9)[b]	5.409(5)	160.3(3)
40.3(3)[a]	5.380(4)	155.7(4)
52.5(9)[b]	5.327(2)	151.1(2)
62.5(1.2)[b]	5.293(4)	148.2(3)
63.1(9)[a]	5.304(5)	149.2(4)
76.0(1.2)[b]	5.232(2)	143.2(2)
85.2(5)[b]	5.214(1)	141.7(1)
89.6(1.0)[a]	5.222(2)	142.4(4)
94.7(2.5)[b]	5.182(4)	139.1(3)
104.2(2.0)[b]	5.171(2)	138.2(2)
124.4(1.1)[b]	5.152(4)	136.7(3)

[a]Third experiment
[b]Forth experiment
[c]Errors were estimated

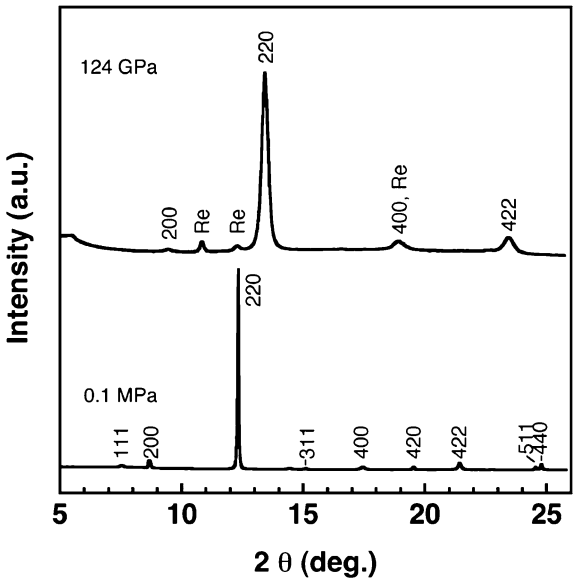

Fig. 2 X-ray diffraction patterns of Fe-17.8 wt% Si with DO_3 structure at 0.1 MPa and 124 GPa at 300 K. A monochromatic beam (wavelength = 0.4256 Å) was used as X-ray source. *Re* rhenium gasket

the data reported by Lin et al. (2003) (Fig. 3b) and appear to shift systematically from the second run. The pressure values were determined by the ruby scale and no internal pressure marker (e.g., Pt, Au) was used in the first run, whereas the equation of state of Pt was used as a pressure scale in the second run. The difference in the P–V data between our first and second runs may be caused by the effect of nonhydrostatic stress. When the experiments were performed without a pressure medium, the EOS parameters obtained were strongly dependent on the degree of nonhydrostatic stress in the sample (Merkel et al. 2002) or the experimental condition. There is also a possibility that the pressure of the area exposed with X-ray beam was overestimated because only one ruby chip was located in the center of the anvil. The EOS parameters given by fitting to the P–V data of the second run are the bulk modulus (K_0) of 198(9) GPa and the first pressure derivative of the bulk modulus (K'_0) of 4.7(3). Although these results are different from the values obtained by Lin et al. (2003) (Fig. 3b), it seems to be caused by the tradeoffs between K'_0 and K_0 and both data themselves are consistent with each other.

The volume of the hcp phase at zero pressure, V_0, given from the second experiment is 22.3(8) Å^3, compatible with the value reported by Lin et al. (2003); $V_0 = 22.21(5)$ Å^3. ΔV for the phase transition, interpolated to zero pressure, is 0.70 Å^3. The volume difference of 3.0% for bcc–hcp phase transformation, $[V(\text{bcc})–V(\text{hcp})]/V(\text{bcc})$, is slightly smaller than that of iron, 5.1% (Mao et al. 1990).

The volumes of bcc phase with Fe-8.7 wt% Si in this work are significantly larger than that of the recent X-ray diffraction measurement using both a DIA-type cubic anvil apparatus and DAC (Zhang and Guyot

Fig. 3a–c Pressure–volume relations for **a** bcc Fe-8.7 wt% Si, **b** hcp Fe-8.7 wt% Si, and **c** Fe-17.8 wt% Si. Compression data for bcc– and hcp—$Fe_{85}Si_{15}$ (7.9 wt% Si) and $Fe_{71}Si_{29}$ (17.0 wt% Si) reported by Lin et al. (2003) are also plotted (*open circles*). **a** *Solid circles* and *solid squares* show the first and the second runs, respectively. *Open triangles* are the data from Zhang and Guyot (1999). *Solid, dashed* and *dotted lines* represent a third-order Burch–Murnaghan equation of state (BM EOS) fitted to our data, Zhang and Guyot (1999), and Lin et al. (2003), respectively. **b** *Solid circles* and *solid squares* show the first and the second runs, respectively. *Solid* and *dotted lines* show a third-order BM EOS fitted to our data in second run and the data reported by Lin et al. (2003), respectively. **c** *Solid* and *dotted lines* represent a third-order BM EOS fitted to our data and the data reported by Lin et al. (2003), respectively. The volume data from Lin et al. (2003) (*open circles*) multiplies the raw data by eight (see text in detail). The equation of state is dependent on the stress conditions in the sample. Iron–silicon alloys appear less compressible in the nonhydrostatic experiments

1999; Lin et al. 2003). The bulk modulus, K_0, of 268(5) GPa was obtained, with K'_0 fixed to 5.3 in order to compare with previous studies. The K_0 for the bcc phase is much higher than the values reported by Zhang and Guyot (1999) and Lin et al. (2003) (Fig. 3a). This discrepancy is due to the nonhydrostatic effect in DAC, which generally causes higher values of K_0 and/or K'_0 (Guyot et al. 1997; Merkel et al. 2002). In the study of Lin et al. (2003), the sample was annealed by an external heating method to reduce the effects of nonhydrostatic stress. In general, nonhydrostatic conditions of experiments could lead to overestimation of the volume at given pressure (Singh and Balasingh 1994; Singh et al. 1998).

For Fe-17.8 wt% Si, the bulk modulus and the pressure derivative of the bulk modulus determined by least-squares fit were $K_0 = 207(15)$ GPa and $K'_0 = 5.1(6)$, which were in agreement with the values reported by Lin et al. (2003), where $K_0 = 199.0(5.3)$ GPa and $K'_0 = 5.66(61)$. The bulk modulus determined by the static compression method is consistent with that determined by the shock compression of the alloy with a similar composition, Fe-19.8 wt% Si; $K_0 = 208(10)$ GPa, which was calculated from linear fit to the shock velocity – particle velocity (u_s–U_p) data given by Balchan and Cowan (1966).

The measurements on the bcc phase of Fe-8.7 wt% Si in this work have suffered from strong nonhydrostaticity. They therefore lead to apparent high values of K_0 and/or K'_0 (Guyot et al. 1997; Merkel et al. 2002). The values of K_0 for bcc Fe-8.7 wt% Si are higher than those measured in the studies of Zhang and Guyot (1999) and Lin et al. (2003) that were conducted under more hydrostatic conditions. For hcp-Fe-8.7 wt% Si and Fe-17.8 wt% Si, although there was the effect of nonhydrostatic stress, the problem of nonhydrostaticity would not be so severe since the pressure range investigated extends to very high pressures at which the relative importance of nonhydrostatic stresses is small. However, we cannot rule out that our bulk moduli of Fe–Si alloys are overestimated due to a high stress in the sample

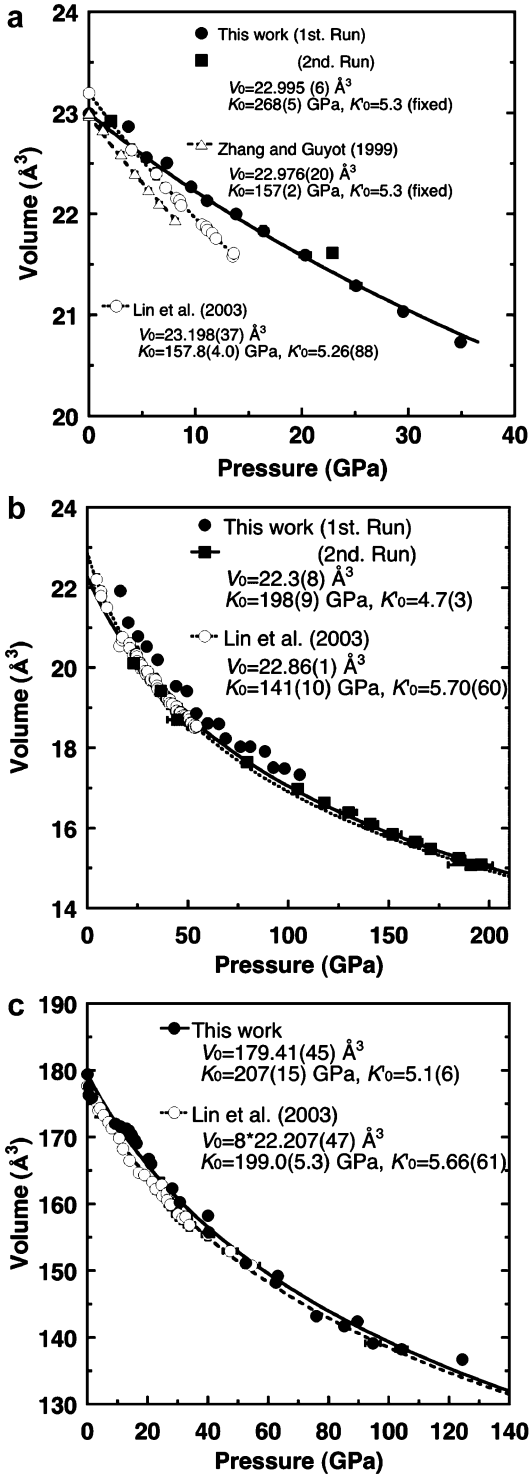

without pressure medium, although the alloys are less compressible than hcp–iron when we compare our compression data of Fe–Si alloys with those of hcp–Fe determined without pressure medium by Mao et al. (1990).

The bulk moduli of iron–silicon alloys obtained in the present study are higher than that of the other iron compounds (Table 4). The EOS parameters of FeS (VI) and FeO (NiAs phase) in Table 4 are corrected from

Table 4 Equation of state parameters for iron compounds

Iron compounds	K_0 (GPa)	K'_0
bcc–Fe-8.7 wt% Si[a]	268(5)	5.3 (fixed)
hcp–Fe-8.7 wt% Si[aj]	198(9)	4.7(3)
Fe-17.8 wt% Si[a]	207(15)	5.1(6)
ε-FeSi[b]	209(6)	3.5(4)
ε-FeSi[c]	184.7(3.9)	4.75(61)
hcp–Fe[d]	164.8(3.6)	5.33(9)
hcp—$Fe_{0.8}Ni_{0.2}$[d]	175(2)	4.95(9)
FeH[e]	121(19)	5.31(0.9)
Fe_3C[f]	174(6)	4.8(8)
FeS (VI)[gi]	74(8)	4 (fixed)
FeO (NiAs phase)[hi]	196(15)	4.3(6)

[a]This work; [b]Knittle and Williams (1995); [c]Lin et al. (2003); [d]Mao et al. (1990); [e]Badding et al. (1991); [f]Li et al. (2002); [g]Fei et al. (1995); [h]Fei and Mao (1994)
[i]Values corrected using $dK_0/dT = -0.04(1)$ GPa and dK'_0/dT is constant
[j]EOS parameters obtained by fitting to the data on second experiment

values at 800 and 900 K to those at 300 K, respectively (Fei et al. 1995; Fei and Mao 1994), by assuming that the value of dK/dT at zero pressure for iron and iron alloys is about –0.04 GPa K^{-1} (Guyot et al. 1997; Dubrovinsky et al. 1998; Zhang and Guyot 1999; Uchida et al. 2001). The large K_0 values for Fe–Si alloys are consistent with those obtained by Knittle and Williams (1995) using DAC (Table 4).

The variation of c/a for the hcp phase, a high-pressure phase of Fe-8.7 wt% Si, obtained in this study is shown in Fig. 4, together with the values for hcp–iron. The axial ratio of hcp Fe-8.7 wt% Si increases slightly with increasing pressures, which is different from that of the hcp phase of pure iron (Jephcoat et al. 1986; Mao

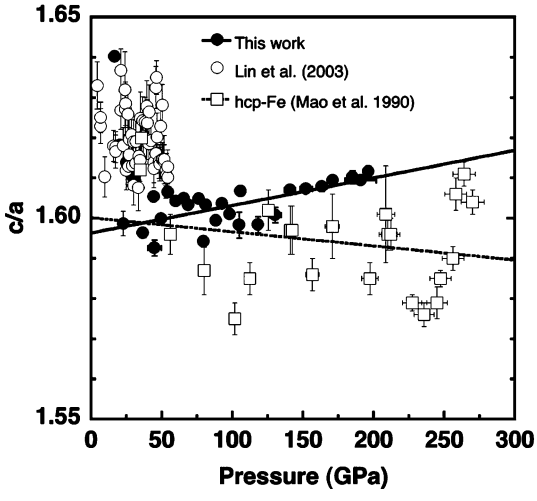

Fig. 4 Plot of the variation of c/a for hcp Fe-8.7 wt% Si as a function of pressure, together with the c/a of hcp iron (Mao et al. 1990). *Solid circles, open circles*, and *open squares* are the data from this work, Lin et al. (2003), and Mao et al. (1990), respectively. The *solid line* indicates the curve fitted linearly above 60 GPa, $c/a = 1.596(2) - 6.8(1.8) \times 10^{-5} \cdot P$. The *dashed line* is the linear fit to data from Mao et al. (1990) for hcp iron

et al. 1990). The values reported by Lin et al. (2003) are larger than those in the present study.

Discussion

Density under inner core condition

In order to compare the results in this work with seismological data (PREM) (Dziewonski and Anderson 1981), the density using the EOS of hcp Fe-8.7 wt% Si was extrapolated to inner-core conditions. First, the experimental P–V curve was extrapolated to inner-core pressure along the 300 K isotherm (Fig. 5). The 300-K isotherm was then thermally expanded to 4000 to 7000 K. Temperature at ICB estimated from melting temperature of pure iron varies and remains uncertain (Brown and McQueen 1986; Williams et al. 1987; Boehler 1993; Yoo et al. 1993). The thermal expansion of hcp Fe-8.7 wt% Si is assumed to be the same as that of hcp iron. The difference in thermal expansions of iron and its alloys is comparatively minor under core pressures (Williams and Knittle 1997). Anderson et al. (1967) showed that the pressure dependence of the thermal expansion coefficient can be expressed in the form $\alpha = \alpha_0 (V/V_0)^n$. Using $\alpha_0 = 5.5 \times 10^{-5}$ K^{-1} (Uchida et al. 2001) and $n = 6.5$ (Boehler et al. 1990; Dobson et al. 2003) for pure iron and the compression data of hcp Fe-8.7 wt% Si, the value of α at the inner-core boundary (ICB) pressure of 330 GPa is estimated to be 2.1×10^{-6} K^{-1}, close to the value used by Dobson et al. (2003). Assuming the temperature of 6000 K at ICB, the correction for thermal expansion at ICB is estimated as $\alpha T = 1.3 \times 10^{-2}$. The density of hcp Fe-8.7 wt% Si deduced from the present experiments is 12.6(5) g cm^{-3} at 330 GPa and 300 K. Using the correction, the density of hcp Fe-8.7 wt% Si is obtained to be 12.5(4) g cm^{-3} at 330 GPa and 6000 K.

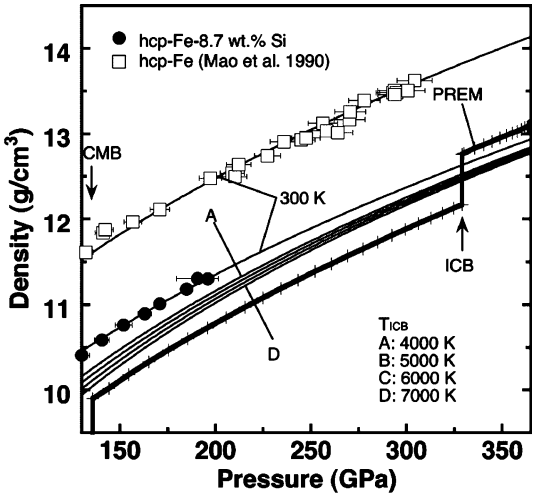

Fig. 5 Density at core pressures and temperatures for hcp Fe-8.7 wt% Si, hcp iron (Mao et al. 1990), and PREM (Dziewonski and Anderson 1981). *Solid circles* and *open squares* are the data from this work and Mao et al. (1990), respectively. The *curves* for hcp Fe-8.7 wt% Si and hcp iron are extrapolated using the third-order Burch–Murnaghan equation of state

For hcp iron, Mao et al. (1990) estimated the density of 13.8(1) g cm^{-3} at 330 GPa and 300 K, which is 9% denser than hcp Fe-8.7 wt% Si. The same procedure yields α of 2.0×10^{-6} K^{-1} and the density of 13.6(1) g cm^{-3} for hcp iron at 330 GPa and 6000 K. The density at ICB deduced from the seismological data is 12.76 g cm^{-3}. Therefore, the density of PREM is about 6% lower than that of hcp iron at ICB and 6000 K. Using the calculation by Poirier (1994), a solubility of a light element in iron can be estimated (see Appendix in Poirier 1994). Considering the light element in iron as silicon, we estimate the value of 4–9 wt% at 6000 K for the mass fraction of silicon compatible with a core density deficit. Even if the amount of silicon in inner core is calculated assuming the temperature of 4000, 5000, and 7000 K at ICB, the silicon content in the core is estimated within 3–10 wt%. It is consistent with that estimated by Dobson et al. (2003) and Lin et al. (2003) for the inner core.

Bulk sound velocity calculation

The bulk sound velocity of pure liquid iron appears to be about 10% lower than those of the PREM core (Anderson and Ahrens 1994). It is likely that the bulk sound velocity of iron–silicon alloys is higher than that of iron under the core condition (Lin et al. 2003). The bulk sound velocity is defined as $V_\phi = (K_s/\rho)^{1/2}$, where ρ is density and K_s is the adiabatic bulk modulus. K_s can be calculated using $K_s = K_T(1 + \alpha\gamma T)$, where the Grüneisen parameter γ is assumed to be between 1 and 2 (Dobson et al. 2003) and the thermal expansion coefficient α is estimated from $\alpha = \alpha_0 (V/V_0)^n$ with $\alpha_0 = 5.5 \times 10^{-5}$ K^{-1} (Uchida et al. 2001) and $n = 6.5$ (Boehler 1990; Dobson et al. 2003). Assuming that the second and higher-order pressure derivatives of the bulk modulus are negligible, K_T and K'_T are calculated using $K_T = K_0 + (\partial K_T/\partial T)_P(T - 300)$ and $K'_T = K'_0$, where K_0 and K'_0 are taken at zero pressure. The temperature derivative of the bulk modulus $(\partial K_T/\partial T)_P$ of -4.48×10^{-2} GPa K^{-1} for hcp iron is used (Uchida et al. 2001). No correction of K'_T for temperature is made because the temperature derivative of K'_T, $(\partial K'_T/\partial T)_P$, has only been estimated for a few materials. These values of α, γ, and $(\partial K_T/\partial T)_P$ for hcp Fe-8.7 wt% Si are assumed to be the same as that of hcp iron. This assumption may be reconciled from the similarity of the thermal expansion and $\partial K/\partial T$ at the ambient conditions for α-$Fe_{0.91}Si_{0.09}$, ε-FeSi, and hcp–Fe in spite of a large difference in the bulk modulus values (Zhang and Guyot 1999). Fig. 6a shows a plot of K_S as a function of pressure under core condition. The bulk modulus K_S is computed assuming the temperature of 4000, 5000, 6000, and 7000 K at ICB. The bulk modulus of hcp–Fe-8.7 wt% Si is higher than that of the PREM inner core,

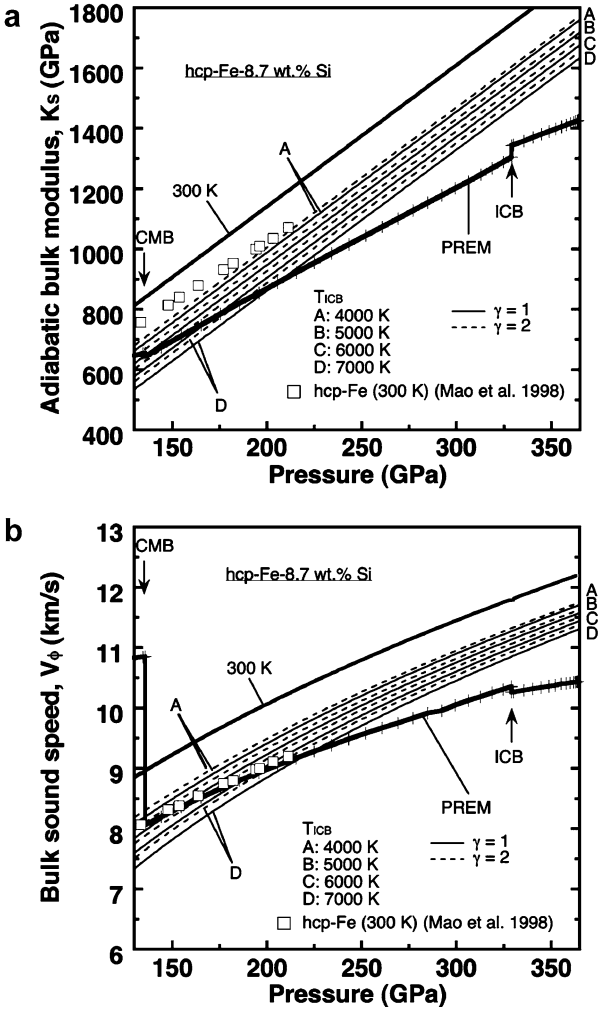

Fig. 6 **a** The adiabatic bulk modulus and **b** the bulk sound velocity of hcp Fe-8.7 wt% Si as a function of pressure at 4000 to 7000 K, compared with that of hcp–Fe and PREM. *Solid* and *dotted curves* for each temperature represent the uncertainty introduced by Grüneisen parameter, γ, to vary between 1 and 2, respectively. The adiabatic bulk modulus and the calculated bulk sound velocity for the pure hcp–Fe (Mao et al. 1998, 1999) are also shown as *open squares*

even if the ICB temperature is assumed to be 7000 K. The calculated bulk sound velocities of hcp–Fe-8.7 wt% Si are also higher than that of the PREM under core condition (Fig. 6b). The reduction of silicon in hcp iron would lead the decrease of the bulk sound velocity for iron (Lin et al. 2003). In order to estimate the Si content in the inner core which can account for the bulk sound velocity of the inner core, we assumed a linear relation between the Si content and bulk sound velocity in hcp Fe–Si alloys up to the Si content of 8.7 wt% Si. If the amount of silicon in hcp iron were 2–5 wt%, the bulk sound velocity of iron–silicon alloy would be consistent with that of inner core.

Knittle and Williams (1995) denied a possibility of Si as a major light element in the outer core based on the EOS of ε-FeSi. Our results, however, indicate that 3–5 wt% of silicon could explain both the density deficit and the bulk sound velocity of the inner core. Lin et al. (2002) showed that at high-pressure and high-temperature iron–silicon alloy decomposed into a mixture of a Si-poor hcp phase and a Si-rich bcc phase, where Si concentrations are ~8 wt% and ~11 wt%, respectively. Recently, it was suggested that above 60 GPa and at high temperature iron–silicon alloys dissociate into a hcp-structured Si-poor iron and a CsCl-structured (B2) FeSi compound (Dubrovinsky et al. 2003), although no measurements of chemical compositions were made for these phases. These works indicate that an Si-poor hcp-structured phase appears at high pressure and high temperature. If the inner core contains silicon, it may be composed of a hcp-structured phase with a few weight % silicon and/or an Si-rich phase (bcc- and/or B2-structured). Therefore, it is also essential to measure experimentally the elastic properties of iron–silicon alloys with bcc and B2 structure under core conditions in order to constrain the composition of the Earth's core.

Acknowledgements This work is supported by a grant-in-aid for the Scientific Research of Priority Area (no. 12126201) and the Scientific Research (S) (no. 14102009) of Ministry of Education, Culture, Sport, Science, and Technology of Japanese Government to E. Ohtani. X-ray diffraction experiments were performed under the approval of the Photon Factory Program Advisory Committee (proposal numbers: 01G059 and 02G055). We thank L.S. Dubrovinsky and F. Guyot for their careful reviews and comments on the manuscript.

References

Allègre CJ, Poirier JP, Humler E, Hofmann AW (1995) The chemical composition of the Earth. Earth Planet Sci Lett 134: 515–526

Anderson OL (1967) Equation for thermal expansivity in planetary interiors. J Geophys Res 72: 3661–3668

Anderson WW, Ahrens TJ (1994) An equation of state for liquid iron and implications for the Earth's core. J Geophys Res 99(B3): 4273–4284

Badding JV, Hemley RJ, Mao HK (1991) High-pressure chemistry of hydrogen in metals: in situ study of iron hydride. Science 253: 421–424

Balchan AS, Cowan GR (1966) Shock compression of two iron-silicon alloys to 2.7 megabars. J Geophys Res 71: 3577–3588

Birch F (1952) Elasticity and constitution of the Earth's interior. J Geophys Res 69: 227–286

Boehler R (1993) Temperatures in the Earth's core from melting-point measurements of iron at high static pressures. Nature 363: 534–536

Boehler R, Bargen NV, Chopelas A (1990) Melting, thermal expansion, and phase transitions of iron at high pressures. J Geophys Res 95(B13): 21731–21736

Brown JM, McQueen RG (1986) Phase transitions, Grüneisen parameters, and elasticity for shocked iron between 77 and 400 GPa. J Geophys Res 91: 7485–7494

Dobson DP, Crichton WA, Bouvier P, Vocadlo L, Wood IG (2003) The equation of state of CsCl-structured FeSi to 40 GPa: Implications for silicon in the Earth's core. Geophys Res Lett 30(1): 1014 doi: 10.1029/2002GL016228

Drickamer HG, Lynch RW, Clendenen RL, Perez-Albuerne EA (1966) X-ray diffraction studied of the lattice parameters of solids under very high pressure. Solid State Phys 19: 135–228

Dubrovinsky LS, Saxena SK, Lazor P (1998) High-pressure and high-temperature in situ X-ray diffraction study of iron and

corundum to 68 GPa using internally heated diamond anvil cell. Phys Chem Miner 25: 434–441

Dubrovinsky LS, Saxena SK, Tutti F, Rekhi S, LeBehan T (2000) In situ X-ray study of thermal expansion and phase transition of iron at multimegabar pressure. Phys Rev Lett 84: 1720–1723

Dubrovinsky L, Dubrovinskaia N, Langenhorst F, Dobson D, Rubie D, Geßmann C, Abrikosov IA, Johansson B, Baykov VI, Vitos L, Le Bihan T, Crichton WA, Dmitriev V, Weber HP (2003) Iron-silica interaction at extreme conditions and the electrically conducting layer at the base of Earth's mantle. Nature 422: 58–61

Dziewonski AM, Anderson DL (1981) Preliminary reference Earth model. Phys Earth Planet Inter 25: 297–356

Fei Y, Mao HK (1994) In situ determination of the NiAs phase of FeO at high pressure and temperature. Science 266: 1678–1680

Fei Y, Prewitt CT, Mao HK, Bertka CM (1995) Structure and density of FeS at high pressure and high temperature and the internal structure of Mars. Science 268: 1892–1894

Fiquet G, Badro J, Guyot F, Requardt H, Krisch M (2001) Sound velocities in iron to 110 gigapascals. Science 291: 468–471

Gessman CK, Wood BJ, Rubie DC, Kilburn MR (2001) Solubility of silicon in liquid metal at high pressure: implications for the composition of the Earth's core. Earth Planet Sci Lett 184: 367–376

Goarant F, Guyot F, Peyronneau J, Poirier JP (1992) High-pressure and high-temperature reactions between silicates and liquid iron alloy, in the diamond anvil cell, studied by analytical electron microscopy. J Geophys Res 97: 4477–4487

Guyot F, Zhang J, Martinez I, Matas J, Ricard Y, Javoy M (1997) *P–V–T* measurements of iron silicide (ε-FeSi): Implications for silicate-metal interactions in the early Earth. Eur J Mineral 9: 277–285

Hillgren VJ, Gessmann CK, Li J (2000) An experimental perspective on the light element in Earth's core. In: Canup RM, Righter K (eds) Origin of the Earth and the Moon. Univ of Arizona Press, Tuscon AZ, pp 245–263

Holmes NC, Moriarty JA, Gathers GR, Nellis WJ (1989) The equation of state of platinum to 660 GPa (6.6 Mbar). J Appl Phys 66: 2962–2967

Jeanloz R (1990) The nature of the Earth's core. Annu Rev Earth Planet Sci 18: 357–386

Jephcoat A, Olson P (1987) Is the inner core of the Earth pure iron? Nature 325: 332–335

Jephcoat AP, Mao HK, Bell PM (1986) Static compression of iron to 78 GPa with rare gas solids as pressure-transmitting media. J Geophys Res 91 (B5): 4677–4684

Knittle E, Jeanloz R (1991) Earth's core-mantle boundary: results of experiments at high pressures and temperatures. Science 251: 1438–1443

Knittle E, Williams Q (1995) Static compression of ε-FeSi and an evaluation of reduced silicon as a deep Earth constituent. Geophys Res Lett 22: 445–448

Li J, Mao HK, Fei Y, Gregoryanz E, Eremets M, Zha CS (2002) Compressin of Fe_3C to 30 GPa at room temperature. Phys Chem Miner 29: 166–169

Lin JF, Heinz DL, Campbell AJ, Devine JM, Shen G (2002) Iron-silicon alloy in the Earth's core? Science 295: 313–315

Lin JF, Campbell AJ, Heinz DL, Shen G (2003) Static compression of iron-silicon alloys: Implications for silicon in the Earth's core. J Geophys Res 108(B1): 2045 doi: 10.1029/2002JB001978

MacDonald GJF, Knopoff L (1958) On the chemical composition of the outer core Geophys J 1: 284–297

Mao HK, Bell PM, Shaner JW, Steinberg DJ (1978) Specific volume measurements of Cu, Mo, Pd, and Ag and calibration of the ruby R_1 fluoresence pressure gauge from 0.06 to 1 Mbar. J Appl Phys 49: 3276–3283

Mao HK, Wu Y, Chen LC, Shu JF, Jephcoat AP (1990) Static compression of iron to 300 GPa and $Fe_{0.8}Ni_{0.2}$ alloy to 260 GPa: implications for composition of the core. J Geophys Res 95: 21737–21742

Mao HK, Shu J, Shen G, Hemley RJ, Li B, Singh AK (1998) Elasticity and rheology of iron above 220 GPa and the nature of the Earth's inner core. Nature 396: 741–743; Correction (1999) Nature 399: 280

Merkel S, Jephcoat AP, Shu J, Mao HK, Gillet P, Hemley RJ (2002) Equation of state, elasticity, and shear strength of pyrite under high pressure. Phys Chem Miner 29: 1–9

Poirier JP (1994) Light elements in the Earth's outer core: A critical review. Phys Earth Planet Inter 85: 319–337

Ringwood AE (1959) On the chemical evolution and density of planets. Geochim Cosmochim Acta 15: 257–283

Sherman DM (1997) The composition of the Earth's core: constraints on S and Si vs. temperature. Earth Planet Sci Lett 153: 149–155

Singh A, Balasingh C (1994) The lattice strains in a specimen (hexagonal system) compressed nonhydrostatically in an opposed anvil high pressure setup. J Appl Phys 75: 4956–4962

Singh A, Balasingh C, Mao HK, Hemley R, Shu J (1998) Analysis of lattice strains measured under nonhydrostatic pressure. J Appl Phys 83: 7567–7575

Song X, Ahrens TJ (1994) Pressure-temperature range of reactions between liquid iron in the outer core and mantle silicates. Geophys Res Lett 21: 153–156

Uchida T, Wang Y, Rivers ML, Sutton SR (2001) Stability field and thermal equation of state of ε-iron determined by synchrotron X-ray diffraction in a multianvil apparatus. J Geophys Res 106(B10): 21799–21810

Wänke H (1981) Constitution of terrestrial planets. Phil Trans Roy Soc Lond (A) 303: 287–302

Williams Q, Knittle E (1997) Constrains on core chemistry from the pressure dependence of the bulk modulus. Phys Earth Planet Inter 100: 49–59

Williams Q, Jeanloz R, Bass J, Stevenson B, Ahrens TJ (1987) The melting curve of iron to 250 gigapascals: a constraint on the temperature at Earth's center. Science 236: 180–181

Wood IG, Chaplin TD, David WIF, Hull S, Price GD, Street JN (1995) Compressibility of FeSi between 0 and 9 GPa, determined by high-pressure time-of-flight neutron powder diffraction. J Phys: Condens Matter 7: L475–L479

Yoo CS, Holmes NC, Ross M, Webb D, Pike C (1993) Shock temperatures and melting of iron at Earth core conditions. Phys Rev Lett 70: 3931–3934

Zhang J, Guyot F (1999) Thermal equation of state of iron and $Fe_{0.91}Si_{0.09}$. Phys Chem Miner 26: 206–211